Journal of the American Ceramic Society

Textured dense Zinc Oxide layers for active noise cancelling windows

Journal:	*Journal of the American Ceramic Society*
Manuscript ID	JACERS-40878
Manuscript Type:	Article
Date Submitted by the Author:	04-Oct-2017
Complete List of Authors:	Lüchtenborg, Jörg; Bundesanstalt fur Materialforschung und -prufung, Ceramic Processing and Biomaterials Kober, Delf; Technische Universitat Berlin Fakultat III Prozesswissenschaften, Fachgebiet Keramische Werkstoffe / Chair of Advanced Ceramic Materials Weber, Alfred; Technische Universitat Clausthal, Institute of Particle Technology Melcher, Jörg; Deutsches Zentrum fur Luft und Raumfahrt, Institute of Composite Structures and Adaptive Systems Guenster, Jens; Bundesanstalt fur Materialforschung und -prufung, Ceramic Processing and Biomaterials
Keywords:	zinc oxide, texture, films, optical materials/properties

Textured dense Zinc Oxide layers for active noise cancelling windows

Jörg Lüchtenborg[1], Delf Kober[2], Alfred P. Weber[3], Jörg Melcher[4], Jens Günster[1]

1 Federal Institute of Materials Research and Testing, Berlin, Division 5.4 Ceramic Processing and Biomaterials

2 Technical University Berlin, Berlin, Institut für Werkstoffwissenschaften und Technologien, Fachgebiet Keramische Werkstoffe / Chair of Advanced Ceramic Materials

3 Clausthal University of Technology, Clausthal-Zellerfeld, Institute of Particle Technology

4 Deutsches Zentrum für Luft- und Raumfahrt (DLR), Institute of Composite Structures and Adaptive Systems, Braunschweig

Abstract

Dense ZnO films with a strong c-axis texture have been deposited on TCO-Glass, Glass and Si wafers, respectively, with a two-step pressureless wet chemical method using zinc acetate dihydrate as Zn-precursor. The crystallographic structure of the films has been studied with XRD and SEM. Optical measurements reveal a high transparency of the ZnO films with a thickness of up to 10 µm. This new cost effective route for ZnO film deposition does not require expensive sophisticated equipment and is easily upscaled.

1. Introduction

ZnO has attracted considerable attention because of its interesting properties. It is a semiconductor material with a direct band gap of 3,37eV and an exciton binding energy of 60 meV at room temperature[1]. Its advantageous use is based on its low-cost, abundant availability and its environmental friendliness. Furthermore, it is biosafe for medical and environmental applications and biocompatible[2]. ZnO crystallizes in hexagonal wurzite and

cubic zinc blend structure whereby the hexagonal phase, which space group is $P6_3mc$, is the most abundant form. Because there is no center of inversion in the crystal structure ZnO is piezoelectric. It is transparent in the visible wavelength range and has photocatalytic properties.

Many efforts have been put into research of ZnO for applications like Acoustic wave filters[3], Photonic crystals[4], Photodetectors[5], Light emitting diodes[6], Photodiodes[7], Gas sensors, Solar cells[8], Varistors[9].

The present work is particularly motivated by the combination of the two physical properties piezo electricity and optical transparency, making ZnO an excellent candidate for the use as a coating on conventional window panes for active noise cancellation. Previous concepts of active noise cancellation in windows were based on the use of actuators, basically loudspeakers, which have been positioned between the individual glass panes of a window. These concepts never found their way into the market because of their disadvantages: they need 3 panes and the distance between the both inner panes is too large. An alternative approach is based on transparent and active actuator layers at least on one of the glass panes, whereas ZnO is a promising candidate as the functional material in the active layer[10]. A piezoelectric ZnO layer has been proposed to be sandwiched by transparent conductive oxide (TCO) electrodes and deposited on a transparent substrate like glass as depicted in Fig. 1.

In an actively controlled window it is not necessary to dissipate the energy of the incoming sound. Though this energy dissipation would be of obvious advantage for the neighborhood it would require substantial mechanical energy transferred by an active layer into the glass pane. Considering the relative low electro-mechanical efficiency of ZnO compared to PZT[11]

(ZnO: d_{33} = 12.4 pC/N, k_{33} = 0.48; PZT: d_{33} = 500 pC/N, k_{33} = 0.69) this would result in an uneconomic electrical power installation. Instead, an actively controlled reflection coefficient of r=-1 guarantees the total reflection of the sound at a significantly reduced power consumption. An adaptive controller adjusts the ZnO-actuator layer as an infinite soft wall. The acoustic impedance of the window is zero. No sound will be transmitted to the interior. Besides a sophisticated electronic feedback loop, this approach requires an active actuator layer at least at certain positions or better over the entire surface of a glass pane.

There exists a considerable body of literature on synthesis and application of ZnO nanowires and nanorods, deposited as layers of well separated crystallites with high c-axis (0001) orientation on various substrates. On the other hand, little research is devoted to the generation of dense and thick (>10 µm) ZnO films. There are reports from sputtered dense ZnO films[12] and other methods like sol-gel[13], PLD[14], CVD[15], but generally these methods have disadvantages intrinsic to the particular coating process, e.g., limitations in substrate size, crystal orientation, use of hazardous and harmful precursors, maximum achievable film thickness or they simply require too costly equipment. With the sol-gel approach a time-consuming repetition of the dip-coating process is necessary to build up layers of a thickness of 1µm. PLD can produce highly orientated layers but only for small substrates. From photovoltaic thin film technology, there exists a vast expertise in large area deposition of ZnO films as transparent conductive oxide (TCO) layers. These technologies are based on chemical vapor deposition (CVD) and generally provide films, which are to a certain extend electrically conductive even without doping with elements, such as boron or aluminum. Moreover, the thickness of the films is typically not exceeding a few micrometers. Electrical insulating properties are, however, required for minimizing ohmic losses during use of the

films as piezo active layers and, thus, application of an electric field. A high density of the films is required for good optical properties, that is, high transmissivity, and for obtaining sufficient in plane stiffness to match the mechanical impedance of film and glass pane. Furthermore, strong texturing with c-axis orientation of the ZnO crystals in the film ensure a good electro-mechanical efficiency[16].

Vayssieres et al.[17] proposed a hydrothermal method to grow nanorods which was improved through the usage of seed layers[18,19,20]. This method was used for the synthesis of nanowires/nanorods. In the present work, this process has been adapted for the deposition of dense ZnO films. A two -step pressureless wet chemical process was developed for the synthesis of films with the desired properties.

2. Experimental

Highly textured and dense ZnO films have been deposited on supporting substrates, such as SnO_2 coated (TCO), uncoated soda lime float glass and Si wafers, by the following method: First the substrates were cleaned ethanol in an ultrasonic bath. SnO_2-coated glass was obtained from Rosenheimer Glass, Rosenheim Germany. In a nucleation step, the samples where dip-coated in a solution consisting of Zinc acetate dihydrate (Sigma Aldrich) and Ethanol and then annealed in a furnace for 30 min at 350 °C in ambient air. In the actual layer deposition step, samples were placed in a growth solution, which is an aqueous solution of zinc acetate dihydrate (Sigma Aldrich) and hexamethylenetetramine (Sigma Aldrich) at normal pressure. The initial solution concentration of the zinc acetate dihydrate and hexamethylenetetramine solution was varied in different experiments between 0.1 M and 0.3 M. However, the concentration changes during the deposition process, as the

reactants are consumed by forming ZnO. The ratio between Hexamethylenetetramine and zinc acetate dihydrate was kept constant at 3:1 during the entire experiment. The temperature during the deposition was 83 °C. After each 120 min, the solution was refreshed. The substrates were removed from the reaction vessel after approximately 12 h, when the desired thickness of up to 10 µm was reached, and rinsed with distillated water to remove any residual salt on the surface. Thinner layers require a shorter deposition treatment, accordingly. The samples were characterized by scanning electron microscopy (SEM, CS4 CamScan) to confirm the morphology and quality of the deposited ZnO films. Images of the films cross-sections prepared by cleaving of the samples and images with a top view from the films surface were taken for measuring the films thickness and to confirm the films quality, also.

Phase and orientation analysis was made by employing a Bruker D8 Advanced X-ray diffractometer with a Co-tube ($\lambda_{K\alpha 1} = 1.78897$ Å, 35 kV and 40 mA) in Bragg-Brentano-geometry. As sample carrier, an eulerian cradle was used. For the θ-2θ-scan phi and chi were fixed to 0°. The 2θ range was between 25 and 90 °2θ with a step size of 0.02 °2θ. For the orientation and mosaicity investigations, the °θ and °2θ were fixed at the Bragg-angle of the hkl-plane of interest. First, a phi scan was carried out between 0 and 358° in steps of 2°. The phi angle with highest intensity was chosen and fixed for a subsequent chi scan. The chi scan was carried out between 0 and 60° in steps of 1°. Since chi scans provide higher measurable angle range for the (002)-peak, chi scans were preferred over the conventional used rocking curve scans. For profile analysis Topas Software from Bruker was used. The peaks were fitted with split-Pseudo-Voigt profile function to get the integral intensity of each peak for Lotgering factor calculation. Commercial available ZnO powder (Riedel-de Haen, purified) was measured as reference with random orientation.

Direct transmittance was measured with a UV3101PC spectrophotometer (Shimadzu Inc., Japan), overall and diffuse transmittance was measured with Lambda 900 (Perkin Elmer Inc., USA) with a step-size of 1nm.

3. Results and Discussion

By a wet chemical deposition process a film of ZnO is grown on different substrates. The reaction mechanism of the deposition process is as follows[21]: Hexamethylenetetramine reacts with the water to form ammonia which supplies the hydroxide ions. Zinc ions are provided by the zinc acetate dehydrate salt which reacts with the hydroxide to zinc hydroxide. The zinc hydroxide finally precipitates out in the growth process to zinc oxide.

$(CH_2)_6N_4 + 6H_2O \rightarrow 6HCHO + 4NH_3$

$NH_3 + H_2O \leftrightarrow NH_4^+ + OH^-$

$2OH^- + Zn^{2+} \rightarrow Zn(OH)_2$

$Zn(OH)_2 \rightarrow ZnO + H_2O$

After deposition, the layers were examined by SEM to get insight into their microstructure and to measure their thickness. First, ZnO was deposited on TCO coated glass without conditioning the surface of the supporting TCO substrate with a seed layer. A representative layer is shown in Fig. 3a, revealing a cross-section image taken by SEM. The concentration of the zinc acetate dihydrate and hexamethylenetetramine solution was 0.1 M with a ratio of hexamethylenetetramine/zinc acetate dihydrate 3:1. No preferred orientation

of the ZnO crystals can be observed. Areas with low density of crystallites and even areas without any obvious crystal growth exist. The average length of the crystallites amounts to 3 µm and their thickness to 1 µm. Since a seed layer should improve the orientation [19, 20], a seeding step was added. In Fig. 3b a similar substrate with the same growth parameters was used but prior to the layer growth step the substrate was dip-coated in a solution of zinc acetate and ethanol and afterwards heat treated for obtaining a seed layer. Now, the deposited layer consists of well oriented ZnO crystallites with a homogenous density, however, the layer is not dense. Well separated individual crystallites can be observed.

Fig. 4 shows SEM images of the cross-section and the top view of the ZnO film grown at different concentrations of the zinc acetate dihydrate and hexamethylenetetramine growth solution. The concentrations of the solution were adjusted to 0.1 M, 0.2 M and 0.3 M. The left hand side of the figure shows the cross sections of the layers together with an approximately 1 µm SnO_2 TCO layer supported by the glass substrate. The ZnO layers have been grown on the TCO layer. The right hand side shows the layers in top down view. The varying concentration of zinc acetate dihydrate and hexamethylenetetramine changes the morphology of the layers significantly. Fig. 4a) and b) show the film grown at a concentration of 0.1 M. The crystallites have a thickness of about 200 nm. Crystallites growing next to each can be found, but also well separated crystallites. In c) and d) the solution concentration of zinc acetate dihydrate and Hexamethylenetetramine is increased to 0.2 M. Thicker crystallites, with a diameter of about 700 nm, are formed. An increase in the concentration leads to increasing crystallites

diameter by a higher concentration of Zn^{2+} ions enhancing the growth of the prismatic faces. The crystallites start to grow into each other, however, pores are still noticeable in the layer. Increasing the concentration to 0.3 M shown in e) and f), leads to the formation of a dense layer, as revealed by visual inspection.

At a concentration of 0.3 M and a deposition time of 12 h it was possible to grow a dense 10 µm thick layer on the TCO glass substrate, which is shown in Fig. 5. The thickness is homogenous and the surface is smooth. In b) some minor contaminations adhering to the layers surface can be recognized. Crystals adhering to the surface or irregularly build into the layer are believed to be a result of a precipitation of crystals in the solution. These crystals floating in the solution attach to the surface of the growing layer and proceed growing at ill-defined orientation.

Fig. 6 reveals SEM cross-sections of ZnO films deposited on the different substrates: a) Si-Wafer b) glass substrate and c) glass substrate with 1 µm SnO_2 TCO coating. The deposition on different substrates leads to no significant change in the morphology of the deposited films. The film on the Si-Wafer is thinner than the films on the glass and the TCO-glass but its internal structure is the same. All films are characterized by ZnO columns growing from the substrate-film interface to the films surface. Apparently, the applied deposition process works independent of the used substrate as it is known for nanorods with zinc nitrate as Zn-precursor [17].

3.1 XRD:

Samples grown on SnO_2-TCO-glass as substrate with a concentration of 0.3 M and different deposition times for obtaining different thicknesses are characterized with XRD. In Fig. 7 the X-ray diffraction patterns of the films with different thicknesses, with initial deposited seed layer, seedless film, and ZnO powder are depicted. The peak intensities of the powder sample match with the powder diffraction file (pdf 89-1397) and indicate random crystallite orientation suitable for the calculation of the Lotgering factor. Patterns of the films show two phase structures: SnO_2 (glass coating as electrode) and the processed ZnO. The relative intensities of the observed peaks in the diffractogram of both phases differ from the Intensities of the pdf-cards, indicating a preferential orientation of the crystallites in the deposited ZnO film as well in the SnO_2 layer. With increasing film thickness a strong increase in the ZnO (002) and (004) peak intensities relative to the SnO_2 signature can be seen. The intensity of the (002) peak ranges from 75cps (1 µm film) to 1630 cps (10 µm film). With increasing ZnO film thicknesses the SnO_2 signal is more and more attenuated, because of the limited probing depth of XRD. For 2 µm and 10 µm with intensities above 500 cps the absorption edge of the used Fe-β-Filter is visible as well as remnant CoK_β radiation from (002)-reflection (◊). For the sample without seed layer the intensities are similar to that of the powder pattern, i.e. the orientation is more random compared to layers grown with seed layer.

Level of orientation

For a semi quantitative estimation of the level of orientation the Lotgering factor (LF) [22] was used. It can be calculated from a $\theta - 2\theta$-scan. In Bragg-Brentano geometry diffraction only

from lattice planes parallel to the sample surface (more correct: with respect to Bragg's law the normal of the lattice plane has to be parallel to the diffraction vector $\vec{q}$) is measured. Its intensity depends on the frequency of the lattice planes oriented parallel to the sample surface. In oriented crystals the frequencies of the individual lattice planes oriented parallel to the sample surface is changing with respect to non-oriented samples and so do their intensities. The Lotgering Factor (LF) is calculated from the Intensities of the a $\theta - 2\theta$-diffractograms with the following equation [22,23]:

$$LF = \frac{p-p_0}{1-p_0} \quad (1)$$

With $= \frac{\sum I_{(hkl)pref}}{\sum I_{(hkl)}}$, the ratio of the intensities of the preferred orientation (hkls with same orientation e.g. 002 and 004 were summed up) to the intensity of all peaks and p_0 the corresponding for an non-oriented ZnO powder sample. Accordingly, a LF of 1 corresponds to perfectly oriented crystallites and of 0 to random orientation. For more reliable results the integral intensities were used. In Fig. 8 the LF for three different orientations vs. the sample thickness is shown. Among the (0 0 l) orientation two additional preferred orientations were observed: (1 0 3) and (1 0 2) which are inclined to the (0 0 2) plane by an angle of 18.4° (a) and 26.6° (b), respectively. From all measured peaks these two planes have the smallest inclination with respect to the (0 0 2)-plane.

The Lotgering factor shows an increasing (0 0 l)-orientation of the ZnO layer with increasing thickness (Table 1). At the beginning of the growth process for a 1 µm thick layer the Lotgering factor is 0.31 and increases to 0.39 for 1.5 µm and reaches 0.76 for a layer of the double thickness of 2 µm. For the ZnO layer with a thickness of 8.5 µm the Lotgering factor is only slightly increased to 0.85. For the sample without seed layer the LF tends to zero, which corresponds to the SEM image in Fig. 3(a). At 1 µm and 1.5 µm, among the (0 0 l) orientation

also the intensities of the crystallographic planes with small inclination (1 0 2) and (1 0 3) to the (0 0 2) are showing considerable intensities, but disappear for layer thicknesses larger than 2 µm. This indicates that for thin layers the ZnO columns are not completely aligned in c-axis orientation perpendicular to the sample surface but inclined to an extent as can be seen in Fig. 4(a). The LF of orientations with bigger inclination with respect to the (0 0 l)-plane are below zero and suppressed compared with the non-oriented powder sample. Additionally, the LF for the samples with different concentration of 0.1 M, 0.2 M and 0.3 M were calculated. The LF is 0.90, 0.87 and 0.87 indicating that the LF is almost independent of the concentration when the ZnO film is thicker than 2.4 µm.

In order to study the mosaicity, that means the slight misorientation of the crystals of the ZnO-film, χ-scans were conducted. In Fig. 9 the χ-scans of the (002)-peak are depicted. They were performed to get a better insight in the orientation distribution of the ZnO-layers. As it is indicated by the $\theta - 2\theta$ scans the intensity is increasing with increasing layer thickness. Conducted φ-scans show constant intensities with varying φ indicating rotation symmetry of the orientation i.e. χ -scan at one φ -angle is sufficient. The orientation distributions are cauchy like. The half width at half maximum are in the range from 8.5° at 1 µm to 6° at 10 µm, i.e. the degree of orientation is increasing with increasing layer thickness, which is in accordance with the Lotgering factor. In Table 1 the thicknesses, LFs, HWHMs and the normalized intensities at χ 18.4° and 26.6° are listed. At these inclination angles of the crystallites to the sample normal Bragg's law is fulfilled for (103) and (102) lattice planes (in Bragg-Brentano geometry with diffraction vector parallel to sample normal). The inset in Fig. 9 shows the trend of these intensities with layer thickness. These intensities are 28 % and 19 % for the 1 µm thick layer and decrease rapidly to 11 % and 4 % at 2 µm. For thicker layers, the decay becomes inferior. It gets obvious that for the two thin layers the (103) and

(102) reflexes, and so, the LF of the (103) and the (102) plane are elevated. The orientation distribution is broader than those from other processing routes reported in literature. With pulsed laser deposition the HWHM are smaller than 3° [14]. For laser ablation smaller than 1° [24] and for solvothermal routes even in range of some tenth arcsec[25]. LF and orientation distribution reveal that in the beginning of the synthesis hexagonal ZnO-crystals grow more randomly distributed. The rod like crystals grow fastest in their c-direction. Crystals which are not perpendicular to the substrate surface will collide with perpendicular growing crystals and get constraint in their further growth. Above 2 µm the crystals growing perpendicular to the surface have suppressed the misoriented, tilted growing crystals. The orientation increases only inferior and the crystals keep on growing.

3.2 Transparency:

Transparency is an important property for an optical device like an active noise cancelling window. The direct transmittance is important for recognizing objects through the window and the total transmittance that means direct and diffuse transmittance is import for the illumination of a room. The transmittance for a laminated sample consisting of SnO_2 substrate, 10 µm ZnO layer and a front glass laminated with EVA foil was measured (Fig. 10). The transmittance starts at 380 nm and reaches 80 % between 550 and 600 nm. The sharp drop for shorter wavelength than 380 nm can be explained by the usage of the EVA foil for the lamination. Diffuse transmittance is shown with the dashed line. The diffuse transmittance has its peak at 400 nm with 60 % and decreases to 20 % at 800 nm. Scattering effects at the ZnO-crystals lying on the surface and the facets (Hace) of the ZnO-layer could be an explanation for this high diffuse transmittance with shorter wavelengths. Direct

transmittance is shown with the dotted line. The direct transmittance gets higher with longer wavelength and reaches 56 % at 800 nm. The total transmittance of the laminated sample is given by the individual transmittances of the components the light is passing through: The used cover glass has a total transmittance of 92 % and the TCO glass without ZnO layer has a total transmittance of 80 %. Although the direct transmittance of the laminated sample is only 56 % the laminated sample can be used for optical applications as can be appreciated from Fig. 11. In Fig. 11 the transparency of the sample is demonstrated. In Fig. 11a the right two-thirds of the sample are with ZnO layer. The building is clearly visible, so that the device could be used as a window.

4. Conclusion

A wet chemical method for the growth of nanowires was adapted for the fabrication of highly c-axis textured ZnO-films with a thickness of up to 10 µm. Increasing the concentration of the zinc acetate dehydrate and Hexamethylenetetramine solution changes the morphology from nanorods to dense layers. The dense layers show a transmittance in the visible range of 80 %. The orientation of the layer is highly c-axis orientated, which is good for piezoelectric applications. The Lotgering factor for a 10 µm thick layer is 0.86. It is found, that thin ZnO layers show little orientation, while texturing is improved with increasing film thickness. This robust process offers the opportunity for the deposition of piezo active and transparent ZnO layers on window panes for an active noise cancelling. Future works will concentrate on the piezoelectric properties of the ZnO layers.

Fig. 1: Possible layer stacking of a piezo active transparent window pane: An active layer (ZnO) is sandwiched between two transparent conductive oxide (TCO) layers acting as electrodes for the use in active noise cancellation.

Fig. 2: Sketch of a Chi-Scan.

Fig. 3: SEM image of a layer cross-sections: a) deposited without seed layer, b) with seed layer

Fig. 4 SEM image of ZnO films grown at different concentrations of the zinc acetate dihydrate and hexamethylenetetramine growth solution. a) cross-section of cleaved samples grown at 0.1 M, b) top view of sample grown at 0.1 M, c) cross-section of sample grown at 0.2 M, d) top view 0.2 M, e) cross-section of sample grown at 0.3 M .

Fig. 5: Cross-section of a cleaved dense layer with a thickness of 10 µm (12 h deposition times in 0.3 M solution)

Fig. 6 Cross-section of the cleaved ZnO films grown on different Substrates. a) Si, b) Glass, c) TCO-Glass.

Fig. 7: XRD patterns of the $\theta - 2\theta$ scans of ZnO layers grown in 0.3 M concentrated solution on TCO glass. Strong preferred (0 0 l)-orientation with peak intensities of 75 cps and 1630 cps for the (002) peak of 1 µm and 10 µm thickness. The inset gives a closer look to the pattern by cutting the upper intensity at 24 cps. For intensities above 500 cps ((002) ZnO peak 2 and 10 µm), the absorption edge of the used Fe-β-Filter and remnant CoK_β (002)-peak (◊) get visible. The SnO_2 phase belongs to the TCO, with preferred orientation, too.

Fig. 8: Lotgering factors for three orientations vs. Layer thickness. The diamonds indicate the Lotgering factors of the sample without seed layer. The LF for the orientations with higher inclination to the 0 0 l orientation are below zero and skipped.

Fig. 9: chi-scans of samples with different layer thicknesses. Chi-scans symmetry was checked at various phi-angles. Half width at half maximum (HWHM, o) and inclination angles of the (103) (a) and (102) planes (b) with respect to (002) are marked. The inset shows the ratio of the intensities at I(a) /I(0) I(b) /I(0) over the layer thickness

Fig. 10: Transmittance of the laminated sample consisting of Substrate SnO_2 glass, 10 µm ZnO layer and a laminated glass slide. The transmission is measured for overall transmittance, direct transmittance and diffuse transmittance.

Fig. 11: View through a 10 µm ZnO layer deposited on TCO glass and laminated with high transparency white glass.

Table 1: Thickness, Lotgering factor, HWHM and normalized intensities for (103) and (102) lattice planes I(a)/I(0) and I(b)/I(0

References

1. Lu F, Cai WP, Zhang YG. ZnO hierarchical micro/nanoarchitectures: Solvothermal synthesis and structurally enhanced photocatalytic performance. *Adv Funct Mater.* 2008;18(7):1047-1056.

2. Zhou J, Xu NS, Wang ZL. Dissolving behavior and stability of ZnO wires in biofluids: A study on biodegradability and biocompatibility of ZnO nanostructures. *Adv Mater.* 2006;18(18):2432-2435.

3. Emanetoglu NW, Gorla C, Liu Y, Liang S, Lu Y. Epitaxial ZnO piezoelectric thin films for saw filters. *Mat Sci Semicon Proc.* 1999;2(3):247-252.

4. Chen YF, Bagnall D, Yao TF. ZnO as a novel photonic material for the UV region. *Mat Sci Eng B-Solid.* 2000;75(2-3):190-198.

5. Liang S, Sheng H, Liu Y, Huo Z, Lu Y, Shen H. ZnO Schottky ultraviolet photodetectors. *J Cryst Growth.* 2001;225(2-4):110-113.

6. Saito N, Haneda H, Sekiguchi T, Ohashi N, Sakaguchi I, Koumoto K. Low-temperature fabrication of light-emitting zinc oxide micropatterns using self-assembled monolayers. *Adv Mater.* 2002;14(6):418-421.

7. Lee JY, Choi YS, Kim JH, Park MO, Im S. Optimizing n-ZnO/p-Si heterojunctions for photodiode applications. *Thin Solid Films.* 2002;403:553-557.

8. Baxter JB, Walker AM, van Ommering K, Aydil ES. Synthesis and characterization of ZnO nanowires and their integration into dye-sensitized solar cells. *Nanotechnology.* 2006;17(11):S304-S312.

9. Lin YH, Zhang ZT, Tang ZL, Yuan FL, Li JL. Characterisation of ZnO-based varistors prepared from nanometre precursor powders. *Adv Mater Opt Electr.* 1999;9(5):205-209.

10. Günster J, Melcher J. Transparent acoustically active device. U.S. Patent US20130322663 A1 2012.

11. Ramadan KS, Sameoto D, Evoy S. A review of piezoelectric polymers as functional materials for electromechanical transducers. *Smart Mater Struct.* 2014;23(3).

12. Joshi S, Nayak MM, Rajanna K. Evaluation. of Transverse Piezoelectric Coefficient of ZnO Thin Films Deposited on Different Flexible Substrates: A Comparative Study on the Vibration Sensing Performance. *Acs Appl Mater Inter.* 28 2014;6(10):7108-7116.

13. Zhang KM, Zhao YP, He FQ, Liu DQ. Piezoelectricity of ZnO films prepared by sol-gel method. *Chinese J Chem Phys.* 2007;20(6):721-726.

14. Serhane R, Abdelli-Messaci S, Lafane S, et al. Pulsed laser deposition of piezoelectric ZnO thin films for bulk acoustic wave devices. *Appl Surf Sci.* 2014;288:572-578.

15. Barnes TM, Leaf J, Fry C, Wolden CA. Room temperature chemical vapor deposition of c-axis ZnO. *J Cryst Growth.* 2005;274(3-4):412-417.

16. Johnson RL. *Characterization of piezoelectric ZnO thin films and the fabrication of piezoelectric micro-cantilevers* [Master], Iowa State University; 2005.

17. Vayssieres L, Keis K, Lindquist SE, Hagfeldt A. Purpose-built anisotropic metal oxide material: 3D highly oriented microrod array of ZnO. *J Phys Chem B.* 2001;105(17):3350-3352.

18. Cui JB, Daghlian CP, Gibson UJ, Pusche R, Geithner P, Ley L. Low-temperature growth and field emission of ZnO nanowire arrays. *J Appl Phys.* 2005;97(4).

19. Song J, Lim S. Effect of seed layer on the growth of ZnO nanorods. *J Phys Chem C.* 2007;111(2):596-600.

20. Zhang YY, Ram MK, Stefanakos EK, Goswami DY. Synthesis, Characterization, and Applications of ZnO Nanowires. *J Nanomater.* 2012.

21. Xu S, Adiga N, Ba S, Dasgupta T, Wu CFJ, Wang ZL. Optimizing and Improving the Growth Quality of ZnO Nanowire Arrays Guided by Statistical Design of Experiments. *Acs Nano.* 2009;3(7):1803-1812.

22. Lotgering FK. Topotactical Reactions with Ferrimagnetic Oxides Having Hexagonal Crystal Structures .1. *J Inorg Nucl Chem.* 1959;9(2):113-123.

23. Furushima R, Tanaka S, Kato Z, Uematsu K. Orientation distribution-Lotgering factor relationship in a polycrystalline material-as an example of bismuth titanate prepared by a magnetic field. *J Ceram Soc Jpn.* 2010;118(1382):921-926.

24. Perriere J, Millon E, Seiler W, et al. Comparison between ZnO films grown by femtosecond and nanosecond laser ablation. *J Appl Phys.* 2002;91(2):690-696.

25. Ehrentraut D, Sato H, Kagamitani Y, Sato H, Yoshikawa A, Fukuda T. Solvothermal growth of ZnO. *Prog Cryst Growth Ch.* 2006;52(4):280-335.

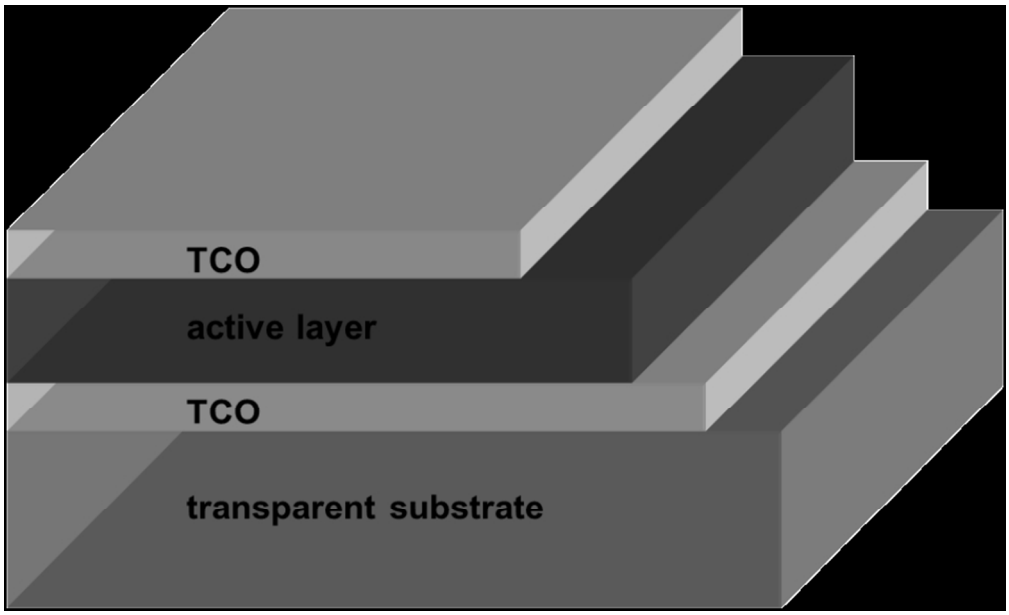

Fig. 1: Possible layer stacking of a piezo active transparent window pane: An active layer (ZnO) is sandwiched between two transparent conductive oxide (TCO) layers acting as electrodes for the use in active noise cancellation.

84x51mm (300 x 300 DPI)

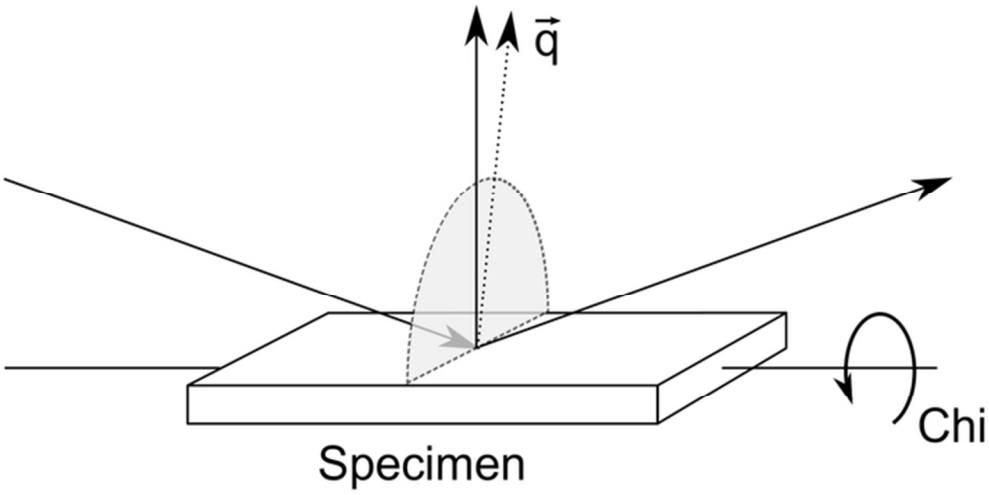

Fig. 2: Sketch of a Chi-Scan.

61x30mm (300 x 300 DPI)

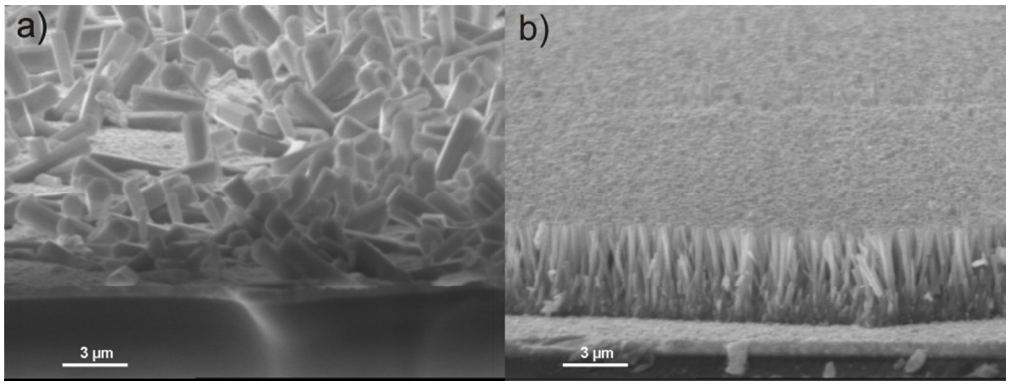

Fig. 3: SEM image of a layer cross-sections: a) deposited without seed layer, b) with seed layer

84x31mm (300 x 300 DPI)

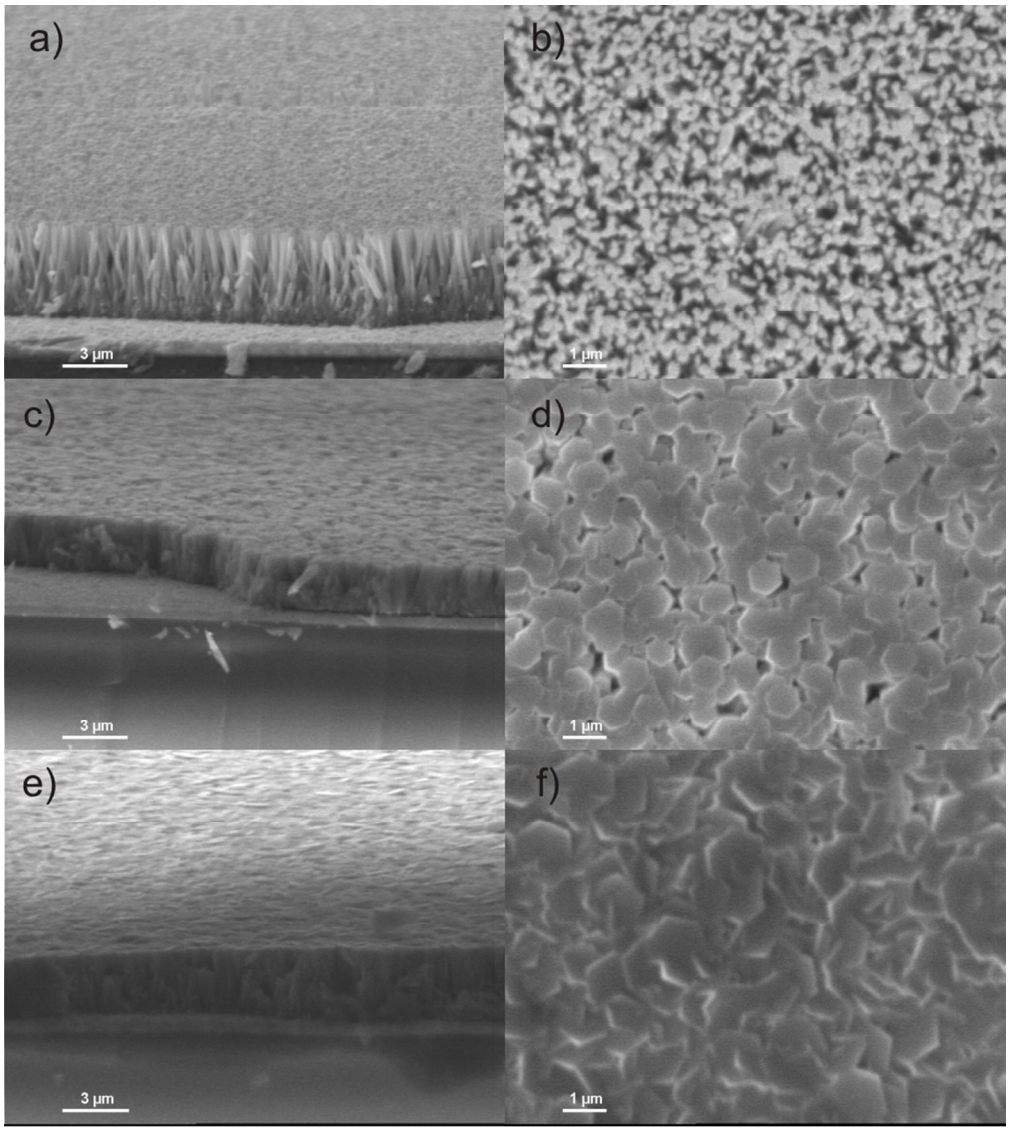

Fig. 4: SEM image of ZnO films grown at different concentrations of the zinc acetate dihydrate and hexamethylenetetramine growth solution. a) cross-section of cleaved samples grown at 0.1 M, b) top view of sample grown at 0.1 M, c) cross-section of sample grown at 0.2 M, d) top view 0.2 M, e) cross-section of sample grown at 0.3 M.

84x95mm (300 x 300 DPI)

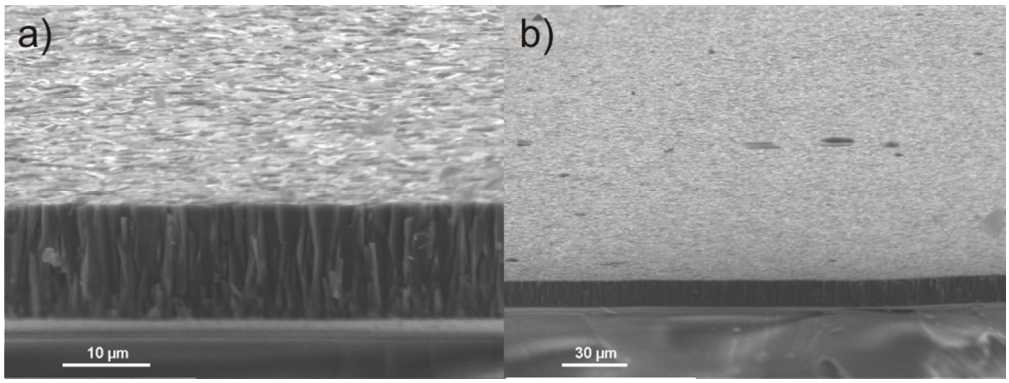

Fig. 5: Cross-section of a cleaved dense layer with a thickness of 10 µm (12 h deposition times in 0.3 M solution)

84x31mm (300 x 300 DPI)

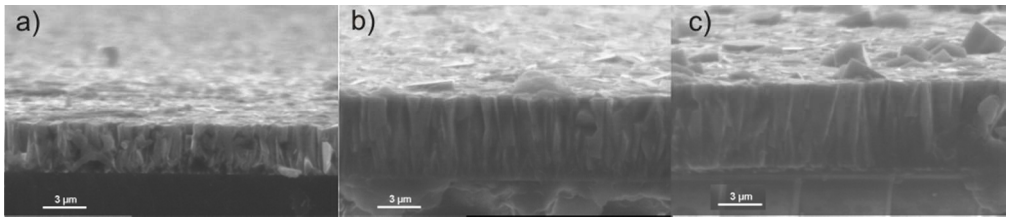

Fig. 6: Cross-section of the cleaved ZnO films grown on different Substrates. a) Si, b) Glass, c) TCO-Glass.

84x17mm (300 x 300 DPI)

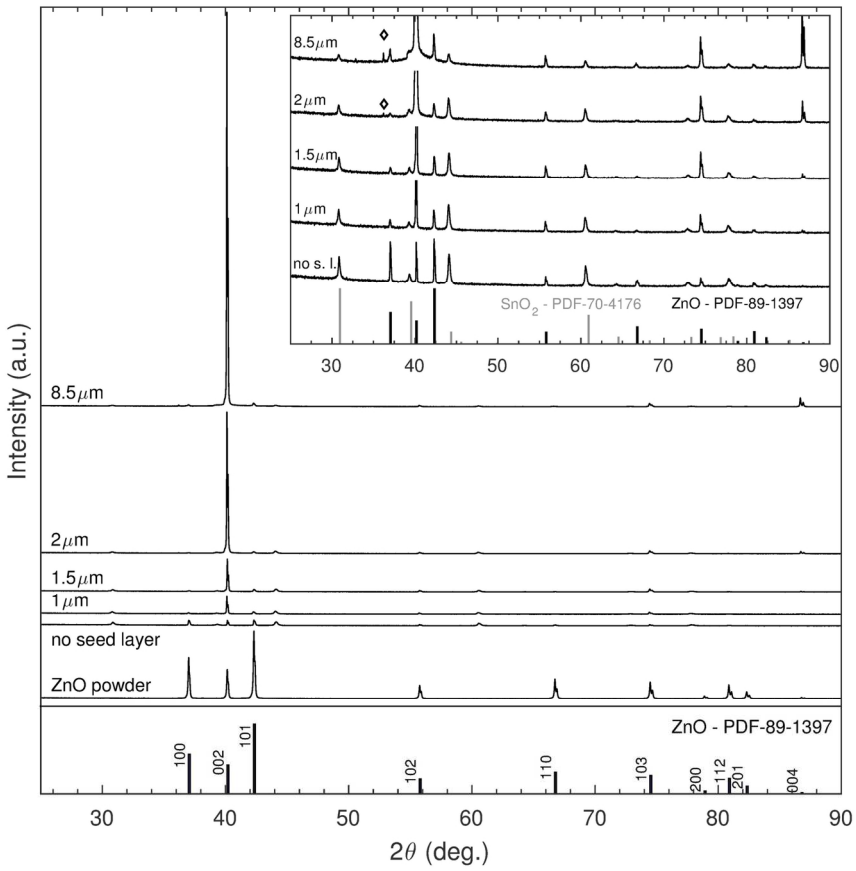

Fig. 7: XRD patterns of the θ-2θ scans of ZnO layers grown in 0.3 M concentrated solution on TCO glass. Strong preferred (0 0 l)-orientation with peak intensities of 75 cps and 1630 cps for the (002) peak of 1 µm and 10 µm thickness. The inset gives a closer look to the pattern by cutting the upper intensity at 24 cps. For intensities above 500 cps ((002) ZnO peak 2 and 10 µm), the absorption edge of the used Fe-β-Filter and remnant CoK_β (002)-peak (◇) get visible. The SnO2 phase belongs to the TCO, with preferred orientation, too.

149x140mm (300 x 300 DPI)

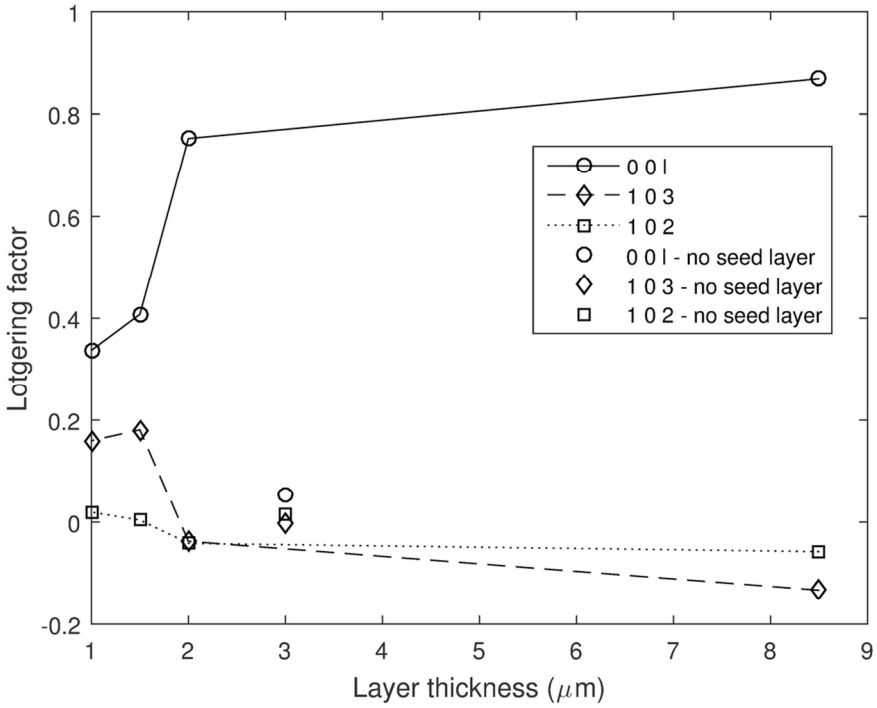

Fig. 8: Lotgering factors for three orientations vs. Layer thickness. The diamonds indicate the Lotgering factors of the sample without seed layer. The LF for the orientations with higher inclination to the 0 0 l orientation are below zero and skipped.

111x83mm (300 x 300 DPI)

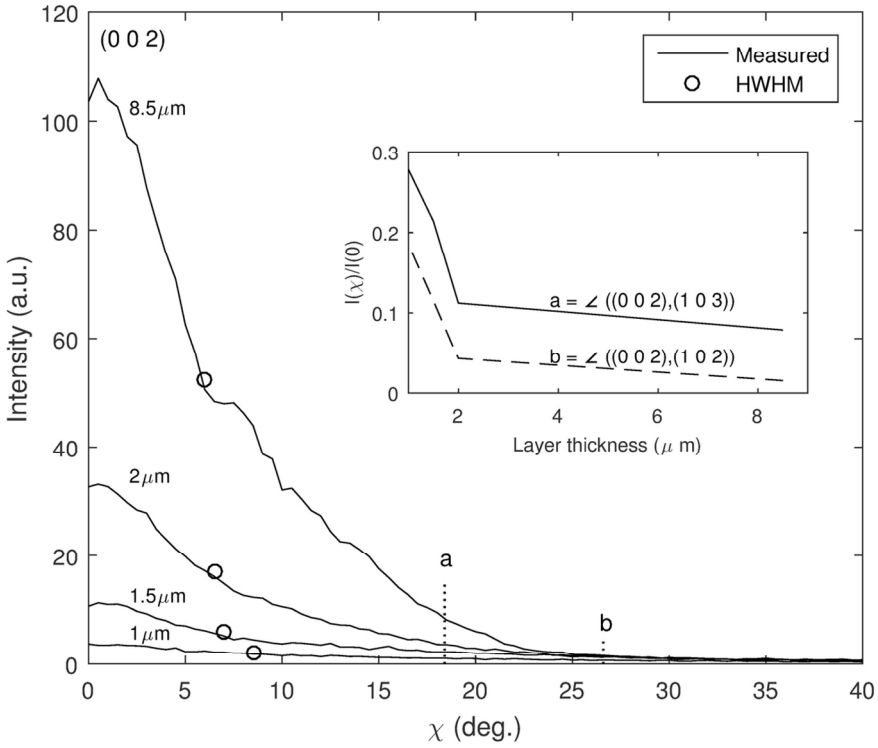

Fig. 9: chi-scans of samples with different layer thicknesses. Chi-scans symmetry was checked at various phi-angles. Half width at half maximum (HWHM, o) and inclination angles of the (103) (a) and (102) planes (b) with respect to (002) are marked. The inset shows the ratio of the intensities at I(a) /I(0) I(b) /I(0) over the layer thickness.

119x95mm (300 x 300 DPI)

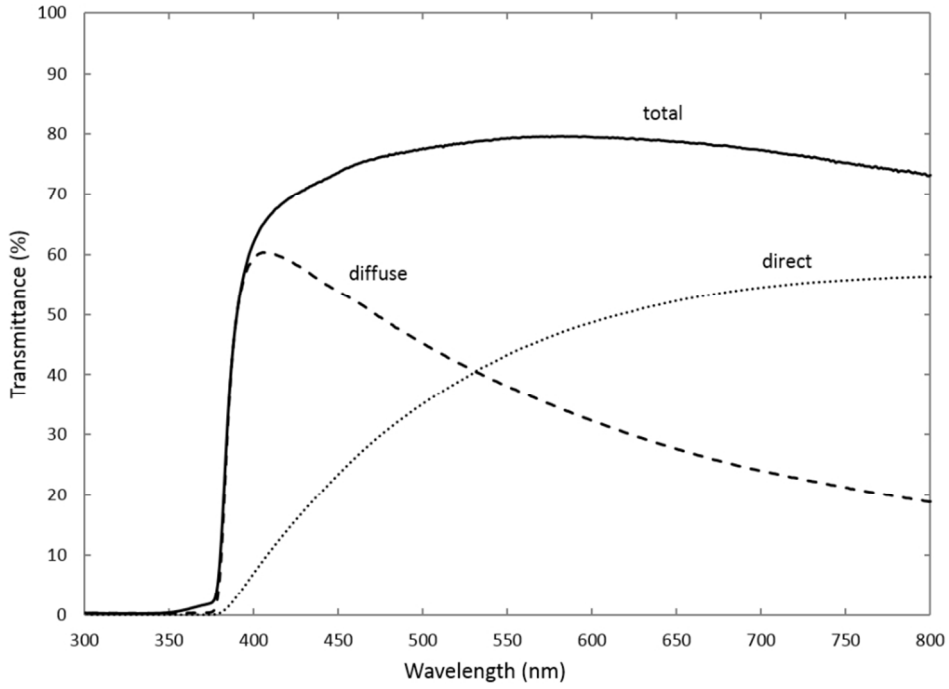

Fig. 10: Transmittance of the laminated sample consisting of Substrate SnO2 glass, 10μm ZnO layer and a laminated glass slide. The transmission is measured for overall transmittance, direct transmittance and diffuse transmittance.

84x59mm (300 x 300 DPI)

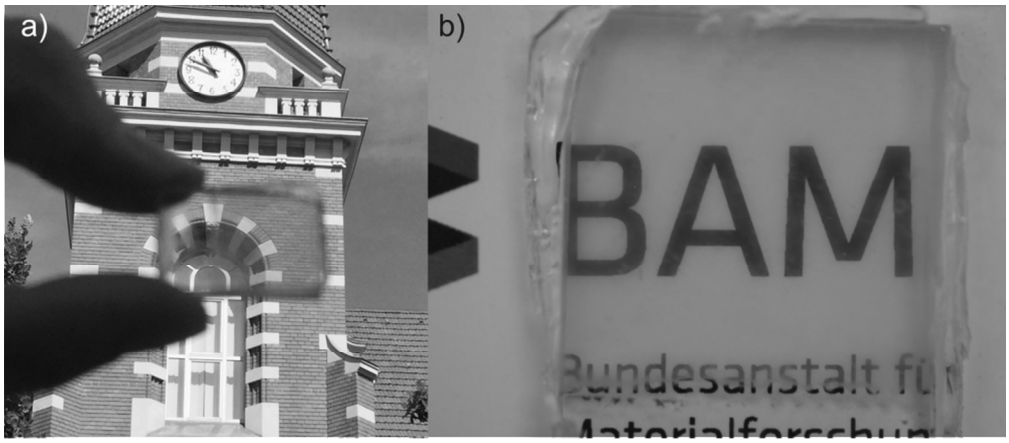

Fig. 11: View through a 10 µm ZnO layer deposited on TCO glass and laminated with high transparency white glass.

84x36mm (300 x 300 DPI)

Table 1: Thickness, Lotgering factor, HWHM and normalized intensities for (103) and (102) lattice planes I(a)/I(0) and I(b)/I(0)

Thickness [µm]	Concentration Mol/l	Lotgering factor (002)	HWHM [deg.]	I(a)/I(0) [%]	I(b)/I(0) [%]
1	0.3	0.31	8.5	27.8	18.5
1.5	0.3	0.39	7	21.4	11.5
2	0.3	0.76	6.5	11.2	4.3
8.5	0.3	0.85	6	7.9	1.5